

Reactions of Sulfur Dioxide with Neutral Vanadium Oxide Clusters in the Gas Phase. I. Density Functional Theory Study[†]

Elena Jakubikova[‡] and Elliot R. Bernstein*

Department of Chemistry, Colorado State University, Fort Collins, Colorado 80523-1872

Received: August 10, 2007; In Final Form: September 17, 2007

Thermodynamics of reactions of vanadium oxide clusters with SO₂ are studied at the BPW91/LANL2DZ level of theory. BPW91/LANL2DZ is insufficient to properly describe relative V–O and S–O bond strengths of vanadium and sulfur oxides. Calibration of theoretical results with experimental data is necessary to compute reliable enthalpy changes for reactions between V_xO_y and SO₂. Theoretical results indicate SO₂ to SO conversion occurs for oxygen-deficient clusters and SO₂ to SO₃ conversion occurs for oxygen-rich clusters. Stable intermediate structures of VO_y (y = 1 – 4) clusters with SO₂ are also obtained at the BPW91/TZVP level of theory. Some possible mechanisms for SO₃ formation and catalyst regeneration for condensed-phase systems are suggested. These results are in agreement with, and complement, gas-phase experimental studies of neutral vanadium oxide clusters.

1. Introduction

Vanadium oxide is a heterogeneous catalyst that plays important roles in catalytic conversion of SO₂ to SO₃,¹ selective oxidation of hydrocarbons,² and selective reduction of NO_x by NH₃.³ Due to the importance of vanadium oxide for industrial scale catalysis, a number of experimental and theoretical studies are devoted to vanadium oxide and its reactivity.

1.1. Experimental and Theoretical Studies of Vanadium Oxide Structure and Reactivity. The electronic and geometrical structures of small vanadium oxide clusters in the gas phase have been investigated by photoelectron spectroscopy,⁴ infrared spectroscopy,⁵ and electron spin resonance spectroscopy.^{6,7} The structure and properties of vanadium oxide clusters also have been studied by means of multireference correlation calculations^{6,8,9} and density functional theory (DFT) calculations.^{10,11}

Gas-phase scattering experiments have been employed to study the reactivity of medium-sized vanadium oxide cations with rare gases, hydrocarbons, and small inorganic molecules.¹² The reactivity of vanadium oxide and vanadium hydroxide cations with hydrocarbons¹³ and methanol¹⁴ was explored by the use of mass spectrometric techniques and DFT calculations. DFT was also applied to study gas-phase reactions of V₂O₅⁺ and V₂O₆⁺ ions with halogenated hydrocarbons,¹⁵ selective catalytic reduction of NO with ammonia on a V₄O₁₆H₁₂ cluster,¹⁶ reactions of VO₂⁺ with C₂H₄ and C₂H₆,¹⁷ and interaction of VO₂⁺ and VO₂⁺ cations with *N*-hydroxyacetamide in aqueous solution.¹⁸

Significant efforts have been devoted to the study of vanadium oxides as nanosized clusters, bulk solid, and clusters supported on different metal surfaces.^{19–25} Extended X-ray absorption fine structure spectroscopies, IR and Raman spectroscopy, as well as DFT calculations, were utilized to study the structure of the

VO₄ molecule as a function of SiO₂, Nb₂O, and ZrO₂ supports.^{19,20} Scanning tunneling microscopy and DFT calculations were used to characterize vanadium oxide nanostructures on the Rh(111) surface.²¹ DFT was employed to investigate the structure and stability of (V₂O₅)_n, n = 1 – 12, gas-phase clusters, and to compare these clusters to the bulk solid V₂O₅.²² Periodic DFT calculations were also applied to study structural and vibrational properties of vanadium oxide aggregates.²³ Furthermore, DFT calculations were utilized to gain insight into the oxidation of methanol to formaldehyde on supported vanadium oxide catalysts²⁴ and oxidative dehydrogenation of propane on vanadium oxide.²⁵

Reduction,²⁶ stability,²⁷ and reoxidation²⁸ of vanadium oxide surface vacancies were studied by means of DFT calculations. Adsorption of oxygen on reduced V₂O₃(0001) surfaces was also investigated by the use of thermal desorption spectroscopy, infrared reflection absorption spectroscopy, high-resolution electron energy loss spectroscopy, X-ray photoelectron spectroscopy, and DFT.²⁹

1.2. Experimental Studies of SO₂ → SO₃ Catalytic Conversion. Although there are currently no reports of vanadium oxide cluster reactivity with SO₂ in the gas phase, catalytic conversion of SO₂ to SO₃ has been studied experimentally over supported vanadium oxide catalysts and in the molten phase. Kato et al.³⁰ investigated a mixture of V₂O₅–K₂SO₄ heated to 500°, 550°, and 600 °C in an atmosphere of SO₂/SO₃/O₂/N₂ gases and determined that reduction of V(V) by SO₂ and oxidation of V(IV) with O₂ are in the equilibrium and the rate determining step of the reaction is the desorption of SO₃ from the molten catalysts into the gas phase.

Dunn and co-workers^{31,32} studied oxidation of SO₂ over supported vanadium oxide catalysts by Raman spectroscopy. They suggested the VO₄ unit attached to the surface has a O=V–(O–M)₃ pyramidal structure, in which O–M represents oxygen–support bonds. They also proposed a catalytic mechanism for SO₃ generation from SO₂ consisting of three steps: (1) adsorption of SO₂ onto V–O–M bridging oxygen; (2) cleavage of the V–O–SO₂ bond and formation of SO₃; and (3) reoxidation of the V atom by dissociatively adsorbed oxygen.

* To whom correspondence should be addressed. E-Mail: erb@lamar.colostate.edu.

[†] Based on a Ph. D. dissertation submitted by Elena Jakubikova to the Department of Chemistry, Colorado State University, 2007.

[‡] Current address: Theoretical Division, Los Alamos National Laboratory, Los Alamos, New Mexico 87544.

The activation energy for this process was determined to be 21 kcal/mol. More recent studies of supported vanadium oxide catalysts suggest that VO₄ is attached to the surface by only one V–O–M bond, and can be described as the chemisorbed O=V–O₂ [oxo] species (“umbrella model”).²⁰

Fouda et al.³³ employed X-ray diffraction techniques, electronic absorption and infrared spectroscopy, and chemical analysis to characterize reaction products of SO₂ → SO₃. The catalyst in this experiment composed of ammonium metavanadate and potassium sulfate. They have identified a mixture of compounds, including compounds of ammonium and potassium polyvanadates, ammonium and potassium bronzes, and ammonium vanadic sulfate. The presence of K₂S₂O₇ in the melt was found to increase catalytic activity of the vanadium based catalyst.

Giakomelou et al. applied in situ Raman spectroscopy to identify vanadium species on the surface of a vanadium oxide based supported molten salt catalyst³⁴ and supported solid V₂O₅/SiO₂ catalyst.³⁵ They found that the distorted tetrahedral O=V–(O–Si)₃ structure is practically inactive, whereas impregnation of the surface with Cs₂SO₄ results in complete structural transformation of the surface and dramatic improvement of SO₂ oxidation.

Multi-instrumental investigation of molten salt/gas model systems and industrial catalysts for SO₂ → SO₃ conversion was undertaken by Lapina and co-workers.¹ They have identified (VO)₂O(SO₄)₄⁴⁺ as the active species and proposed a four step catalytic mechanism consisting of (1) adsorption of O₂ to the active site, (2) first SO₂ → SO₃ conversion, (3) adsorption of second SO₂ molecule, and (4) SO₃ desorption.

Despite the significant effort devoted to the experimental studies, complete understanding of the SO₂ oxidation by vanadium oxide based catalysts is still lacking. The available experimental studies provide different views of the catalytic process, suggesting several mechanisms for SO₂ → SO₃ conversion.

Recently, reactions of neutral vanadium oxide clusters V_xO_y with SO₂ have been studied in the gas phase employing single photon ionization. These studies will be reported in the following experimental paper, referred to as paper II,³⁶ in considerable detail.

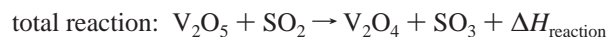
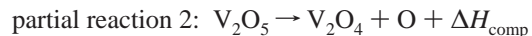
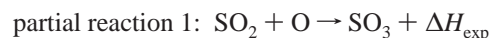
1.3. Goal of This Work. The goal of this work is to study the reactivity of small neutral vanadium oxide clusters, VO_y (y = 1–5), V₂O_y (y = 2–7), V₃O_y (y = 4–9), and V₄O_y (y = 7–12), with SO₂. Our focus lies in investigating the thermodynamics of reactions of vanadium oxides with SO₂. While solid-state studies might provide more realistic models for heterogeneous catalysis, gas-phase metal oxide clusters also represent a valid model for the active sites of the condensed-phase vanadium oxide catalyst.³⁷ Gas-phase experimental and theoretical work have an advantage of being less complex and thus able to provide insights into catalytic processes at the molecular level.

2. Computational Methods

DFT methods have been successfully employed to study structure and reactivity of various metal oxide systems,^{13,15,16} suggesting DFT is a widely accepted tool to study properties of metal oxides. Pykavy and Wüllen⁹ employed multi-reference averaged coupled-pair functional (MR-ACPF) and B3LYP density functional³⁸ to study properties of V₂O₄^{+0/-} species and found good agreement between the MR-ACPF and B3LYP results for molecular structures and the relative energies of different electronic states, as well as for the ionization energies

and the electron affinities. Foltin et al.³⁹ performed benchmark calculations with both BPW91⁴⁰ and B3LYP functionals on zirconium oxides, suggesting BPW91 to be more suitable for computing properties of metal oxides. All calculations described in this work are performed using the BPW91 functional.

Structures of VO_y (y = 1–5), V₂O_y (y = 2–7), V₃O_y (y = 4–9), and V₄O_y (y = 7–12) clusters have been computed at the BPW91/LANL2DZ level of theory and reported in a separate publication.⁴¹ The LANL2DZ basis set⁴² uses Los Alamos effective core potentials with a double-ζ basis set on vanadium atoms, and a D95V basis set⁴³ on oxygen and sulfur atoms. BPW91/LANL2DZ fails to describe bond strengths and other properties of sulfur oxides properly (for more details, see section 3 of Performance of DFT Calculations), therefore experimental enthalpies of formation of sulfur oxides⁴⁴ are used to obtain enthalpies for reactions of vanadium oxides with SO₂. Each reaction of a vanadium oxide cluster with SO₂ is divided into two partial reactions. The first reaction involves oxidation (or reduction) of SO₂, with the enthalpy computed from the experimental enthalpies of formation of sulfur oxides and an oxygen atom. The second reaction consists of reduction (or oxidation) of a vanadium oxide cluster, and the enthalpy for this reaction is calculated from total energies of vanadium oxide clusters and an oxygen atom obtained from calculations performed at BPW91/LANL2DZ level of theory. Total enthalpy for reaction is then computed as the sum of enthalpies for the first and second reactions. To illustrate this on a specific example, the enthalpy for the reaction of V₂O₅ with SO₂ leading to the formation of SO₃ and V₂O₄ is obtained in the following way:



In the above reactions, ΔH_{exp} is obtained from the experimental enthalpies of formation of SO₂, SO₃, and O; ΔH_{comp} is calculated from the BPW91/LANL2DZ energies of the lowest energy isomers of V₂O₅, V₂O₄, and O. Enthalpies are given at 298.15 K. Finally, the total enthalpy of reaction is obtained as a sum of the enthalpies for the two partial reactions: ΔH_{reaction} = ΔH_{exp} + ΔH_{comp}.

To ensure that the LANL2DZ basis set is indeed sufficient to provide reliable description of vanadium oxides, especially when computing the enthalpies of their reactions with SO₂, we have reoptimized lowest energy structures of V₃O_y (y = 4–9) at the BPW91/TZVP level of theory. Enthalpies obtained using the TZVP basis set in combination with the experimental data for sulfur oxides follow the same trends as the enthalpies obtained with LANL2DZ basis set.

Structures of VO_y (y = 1–4) clusters with SO₂ are computed and barriers for reactions of oxygen-deficient VO are also investigated in an effort to learn more about reaction intermediates and reaction paths. Due to the failure of LANL2DZ basis set to provide proper description of sulfur oxides, these calculations are performed at the BPW91/TZVP level of theory using the Gaussian 98 program.⁴⁵

3. Performance of DFT Calculations

3.1. Vanadium Oxides. Table 1 shows the comparison between properties of VO and VO₂ clusters obtained from gas-phase experimental data and properties calculated at different

TABLE 1: Atomization Energies, Bond Lengths, and Structural Parameters for VO and VO₂. All Atomization Energies Reported Here Are Obtained Using ⁴F State of Vanadium Atom

method	VO		VO ₂			
	VO [eV]	V–O [Å]	VO ₂ [eV]	O–VO [eV]	V–O [Å]	O–V–O [deg]
exp.	6.44 ± 0.20 ⁵²	1.589 ⁵³	12.20 ± 0.19 ⁴⁶	5.77 ⁴⁶	1.589 ^{10,54}	110 ^{10,54}
BPW91/LANL2DZ	7.33	1.612	13.13	5.80	1.633	110.99
BPW91/TZVP	7.64	1.586	13.85	6.21	1.612	110.59
BP86/LANL2DZ	7.41	1.611	13.44	6.03	1.632	110.77
BP86/TZVP	7.70	1.585	14.13	6.43	1.611	110.24
BP86/basis limit ⁸	7.46	1.585				
B3LYP/LANL2DZ	6.92	1.607	11.92	4.98	1.627	114.83
B3LYP/TZVP	6.33	1.577	11.75	5.42	1.607	114.63
B3LYP/basis limit ⁸	6.22	1.579				
MR-ACPF/basis limit ⁸	6.44	1.593				
MCPF ⁵⁵	6.06	1.588				
AIMP-MCPF ⁵⁵	6.09	1.586				

levels of theory (density functional as well as ab initio). Density functional methods with the LANL2DZ basis set tend to overestimate bond lengths for VO and VO₂ and the bond angle for VO₂. Use of the TZVP basis set provides better agreement with the experiment, although the calculation still slightly overestimates O–VO bond length, O–V–O bond angle, and underestimates O–V bond length. The hybrid density functional B3LYP tends to underestimate dissociation energies, whereas BPW91 and BP86 overestimate them by about 1 eV. Note that theoretical values for the O–VO bond strength obtained with BP86 and BPW91 functionals employing a LANL2DZ basis set compare rather well to the experimental value of 5.77 eV,⁴⁶ suggesting that the error in atomization energy of VO₂ is carried over from the error in the description of VO. Use of the TZVP basis set with BPW91 and BP86 functionals to compute atomization energies of vanadium oxides does not provide an improvement over the use of a LANL2DZ basis set. BPW91/TZVP overestimates atomization energies of VO and VO₂ by 1.2 and 1.65 eV, respectively, whereas BP86/TZVP overestimates these atomization energies by 1.26 and 1.93 eV, respectively. This is due to the difficulties in obtaining a proper description of the ground electronic state of the vanadium atom, as described in ref 41. Ab initio methods with full electron basis sets, however, tend to slightly underestimate the atomization energies of VO.

From the data presented here, just what method is the best one for calculations of vanadium oxide systems is not entirely clear. While ab initio methods with full electron correlation consistent basis sets provide better accuracy, at this moment they are not practical for use on larger clusters. Density functional methods provide a viable alternative to the ab initio methods; however, one must understand their shortcomings. Additional experimental data are also needed, such as atomization energies and bond strengths of vanadium oxide clusters containing more than one vanadium atom, in order to judge the accuracy of available theoretical methods. We have chosen to use the BPW91 functional, because it provides a correlation component that might be important for proper description of clusters containing more than one vanadium atom, for clusters undergoing reactions, and for calculation of transition states.

3.2. Sulfur Oxides and Oxygen Molecule. Table 2 shows structural parameters for the oxygen molecule and sulfur oxides computed at the BPW91/LANL2DZ and BPW91/TZVP levels of theory. BPW91/LANL2DZ overestimates O–O bond length, whereas BPW91/TZVP provides better agreement with the experiment. Performance of BPW91/LANL2DZ for sulfur oxides is much worse, significantly overestimating S–O bond lengths and underestimating O–S–O bond angle in SO₂

TABLE 2: Bond Lengths and Bond Angles for O₂ and SO_y (y = 1–3)

parameter	exp.	BPW91/LANL2DZ	BPW91/TZVP
O ₂ : O–O	1.208 Å ⁵³	1.288 Å	1.223 Å
SO: S–O	1.4811 Å ⁴⁷	1.653 Å	1.529 Å
SO ₂ : S–O	1.431 Å ⁴⁷	1.636 Å	1.481 Å
SO ₂ : O–S–O	119.329 ^{o47}	113.448 ^o	118.379 ^o
SO ₃ : S–O	1.4198 Å ⁴⁷	1.632 Å	1.467 Å

TABLE 3: Bond Strengths for O₂ and SO_y (y = 1–3)

parameter	exp.	BPW91/LANL2DZ	BPW91/TZVP
O ₂	5.12 ± 0.002 ⁵³	4.90	5.84
O–S	5.40 ⁴⁴	4.16	5.46
O–SO	5.71 ⁴⁴	2.69	5.08
O–SO ₂	3.61 ⁴⁴	1.09	3.24

molecule. This is due to the lack of polarization functions in description of sulfur and oxygen atoms. Use of the TZVP basis set represents an improvement over LANL2DZ and provides acceptable description of bond lengths and bond angles for sulfur oxides, although it still somewhat overestimates sulfur–oxygen bond lengths.

Table 3 compares the experimental atomization energy of the oxygen molecule and the sulfur–oxygen bond strengths of sulfur oxides to the atomization energy and bond strengths obtained from the DFT calculations. Experimental bond strengths of sulfur oxides are obtained from the enthalpies of formation of sulfur and oxygen atoms and SO_y (y = 1, 2, 3) molecules published in NIST Chemistry WebBook⁴⁴ based on consideration of the following reactions: SO → S + O, SO₂ → SO + O, and SO₃ → SO₂ + O. S–O and O–SO bond strengths obtained in this way are in excellent agreement with bond strengths published in CRC Handbook.⁴⁷

BPW91/LANL2DZ provides a surprisingly good value for atomization energy of O₂, which is probably just a coincidence considering that the basis set is of only double- ζ quality and lacks polarization functions. Use of the TZVP basis set to compute atomization energy of O₂ does not provide an improvement over the use of LANL2DZ, overestimating O₂ atomization energy by 0.72 eV.

As can be seen in Table 3, BPW91/LANL2DZ significantly underestimates bonding energies of sulfur oxides, with the largest error being a little over 3 eV for O–SO bond strength. Description of sulfur oxides is dramatically improved by replacing LANL2DZ with the TZVP basis set. The BPW91/TZVP level of theory, however, still underestimates O–SO and O–SO₂ bond strengths and predicts the largest bond strength for S–O, rather than for O–SO. To obtain a proper description

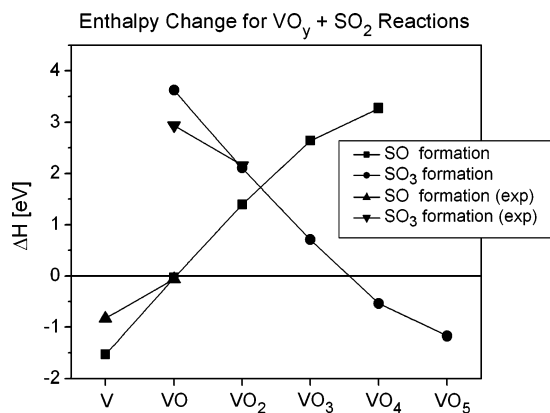
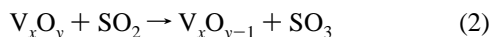
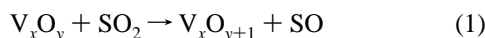


Figure 1. Enthalpy (at 298.15 K) for $\text{VO}_y + \text{SO}_2 \rightarrow \text{VO}_{y+1} + \text{SO}$ (eq 1 in the text) and $\text{VO}_y + \text{SO}_2 \rightarrow \text{VO}_{y-1} + \text{SO}_3$ (eq 2 in the text) reactions.

of sulfur oxide bond strengths, one would need to use a higher level of theory, such as CCSD(T)/cc-pV(X+d)Z ($X = \text{T, Q, 5, 6}$).⁴⁸

4. Results and Discussion

4.1. Thermodynamics of Reactions of Vanadium Oxides with Sulfur Dioxide. Two main reactions of interest occur between V_xO_y clusters and an SO_2 molecule: (1) oxidation of SO_2 and reduction of V_xO_y , resulting in the formation of SO_3 ; and (2) reduction of SO_2 and oxidation of V_xO_y , resulting in the formation of SO . These processes can be generally described by the two following reactions:



To determine which product (SO_3 or SO) is more likely to be formed under the reaction of a particular vanadium oxide cluster with SO_2 , enthalpy changes (at 298.15 K) for both reactions are computed for the lowest energy isomers of VO_y ($y = 1-5$), V_2O_y ($y = 2-7$), V_3O_y ($y = 4-9$), and V_4O_y ($y = 7-12$) clusters.

Figures 1–4 show enthalpy changes for reactions of VO_y ($y = 0-5$), V_2O_y ($y = 2-7$), V_3O_y ($y = 4-9$), and V_4O_y ($y = 7-12$) clusters with SO_2 . The enthalpies of reaction are computed as described in Section 2 (Computational Methods) above, using experimental enthalpies of formation for sulfur oxides and BPW91/LANL2DZ calculations for vanadium oxides. Enthalpies of reactions for the smallest vanadium oxide clusters are also obtained using available experimental enthalpies of formation for vanadium oxides⁴⁷ and are depicted in Figure 1. A comparison of the theoretical and experimental enthalpies of reaction indicates that while the agreement of theoretical and experimental data is not perfect, enthalpy changes obtained from the calculations on vanadium oxides should reproduce general trends.

Computed enthalpy changes for reactions suggest that reactions of oxygen deficient vanadium oxide clusters ($\text{VO}_{0,1}$, V_2O_{2-4} , V_3O_{4-6} , V_4O_{7-9}) with SO_2 result in the formation of SO , while reactions of oxygen rich clusters ($\text{VO}_{4,5}$, $\text{V}_2\text{O}_{6,7}$, $\text{V}_3\text{O}_{8,9}$, $\text{V}_4\text{O}_{11,12}$) with SO_2 lead to the formation of SO_3 . Each series of vanadium oxides also contains clusters, such as VO_2 , V_2O_5 , V_3O_7 , and V_4O_{10} , that are predicted to be stable with respect to the reaction with SO_2 .

These results are in a very good agreement with gas-phase molecular beam experiments performed in our laboratory, in

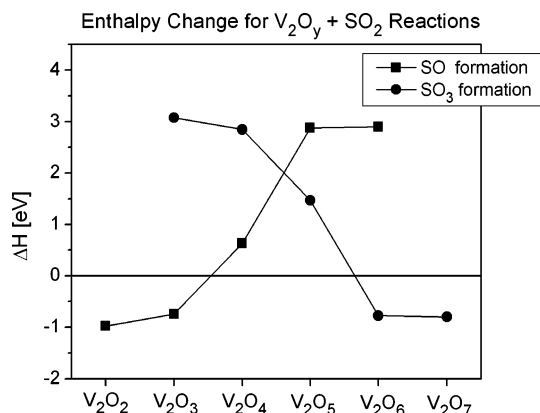


Figure 2. Enthalpy (at 298.15 K) for $\text{V}_2\text{O}_y + \text{SO}_2 \rightarrow \text{V}_2\text{O}_{y+1} + \text{SO}$ (eq 1) and $\text{V}_2\text{O}_y + \text{SO}_2 \rightarrow \text{V}_2\text{O}_{y-1} + \text{SO}_3$ (eq 2) reactions.

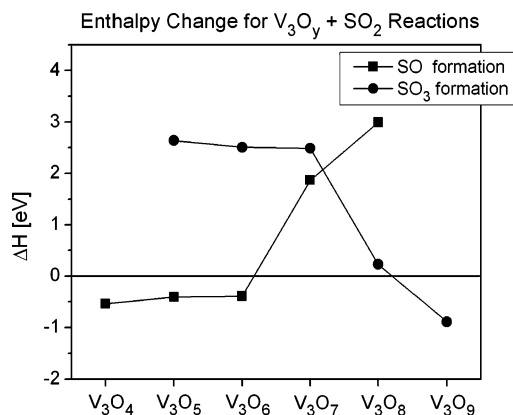


Figure 3. Enthalpy (at 298.15 K) for $\text{V}_3\text{O}_y + \text{SO}_2 \rightarrow \text{V}_3\text{O}_{y+1} + \text{SO}$ (eq 1) and $\text{V}_3\text{O}_y + \text{SO}_2 \rightarrow \text{V}_3\text{O}_{y-1} + \text{SO}_3$ (eq 2) reactions.

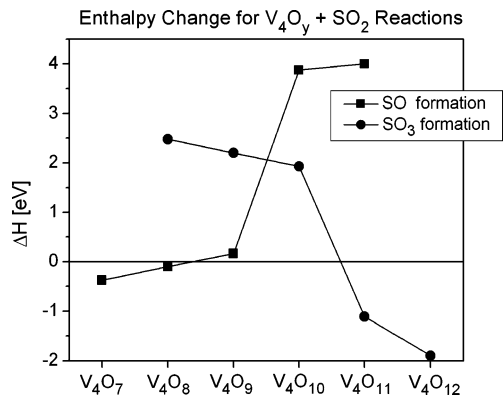


Figure 4. Enthalpy (at 298.15 K) for $\text{V}_4\text{O}_y + \text{SO}_2 \rightarrow \text{V}_4\text{O}_{y+1} + \text{SO}$ (eq 1) and $\text{V}_4\text{O}_y + \text{SO}_2 \rightarrow \text{V}_4\text{O}_{y-1} + \text{SO}_3$ (eq 2) reactions.

which both SO and SO_3 products are observed by 10.5 and 26.5 eV ionization, respectively.³⁶

4.2. Reaction Intermediates, Barriers and Reaction Paths.

In an effort to understand paths for the reactions of vanadium oxides with sulfur dioxide better, intermediate structures of the smallest vanadium oxides, VO_{1-4} , with SO_2 are optimized at the BPW91/TZVP level of theory. Structures of various isomers are depicted in Figures 5–8. The ground electronic states of all of the isomers are doublets, with the exception of the highest energy isomer of VO_2SO_2 , which is a quartet.

Structures of different VO_ySO_2 isomers give some indication of the possible formation of SO , SO_2 , or SO_3 from VO_ySO_2 complexes. The lowest energy structures of VOSO_2 (Figure 5) hint at SO formation, whereas structures of VO_2SO_2 (Figure 6)

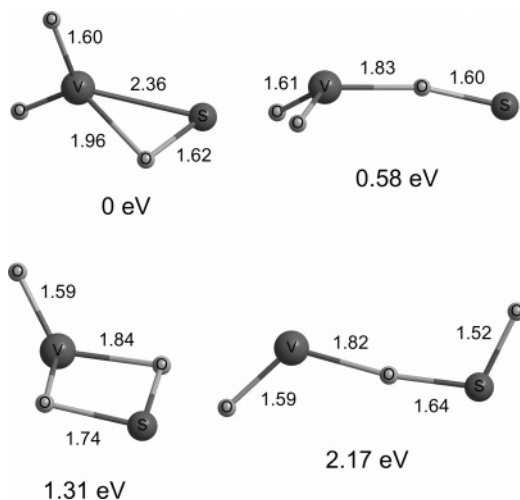


Figure 5. Structures of VOSO_2 computed at the BPW91/TZVP level of theory.

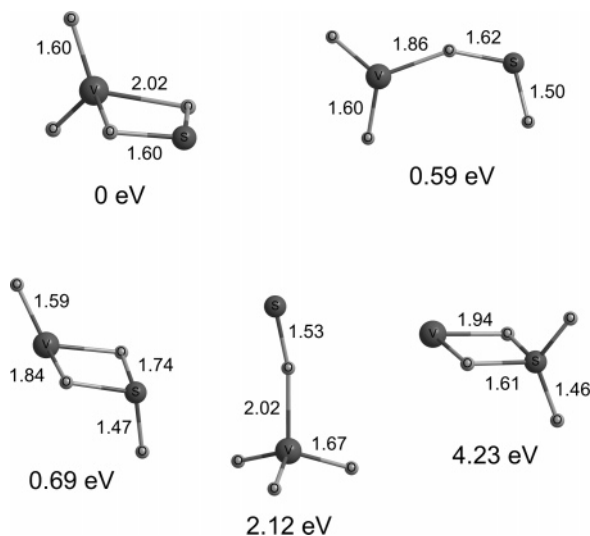


Figure 6. VO_2SO_2 structures computed at the BPW91/TZVP level of theory.

and VO_3SO_2 (Figure 7) are more indicative of SO_2 formation and suggest that VO_2 and VO_3 should be relatively stable with respect to reaction with SO_2 . Low-energy structures of VO_4SO_2 (Figure 8) are, contrary to expectations, also suggestive of SO_2 formation. BPW91/TZVP predicts $\Delta H = +0.62$ eV for the $\text{VO}_4 + \text{SO}_2 \rightarrow \text{VO}_3 + \text{SO}_3$ reaction, whereas BPW91/LANL2DZ calculations calibrated with experimental data for SO_2 predict $\Delta H = -0.54$ eV. The BPW91/TZVP result is a consequence of the overestimation of V–O bond strength and at the same time underestimation of O–SO and O– SO_2 bond strengths. If a better theoretical method were used to optimize these structures, then most probably the same isomers would be obtained, but with different relative energies. This result is nonetheless within the overall ± 1 eV apparent accuracy of the present level of theory.

Table 4 shows the bonding energies of VO_{1-4} with SO_2 for their lowest energy isomers. Even though the bonding energies computed with BPW91/TZVP are probably about 1 eV too strong, we can still conclude that the complexes of V_xO_y clusters with SO_2 should be stable. This is confirmed by the observation of numerous $\text{V}_x\text{O}_y\text{SO}_2$ reaction intermediates in the gas-phase experiments.³⁶

Calculation of a barrier for the reaction of oxygen deficient VO with SO_2 is also performed at the BPW91/TZVP level of

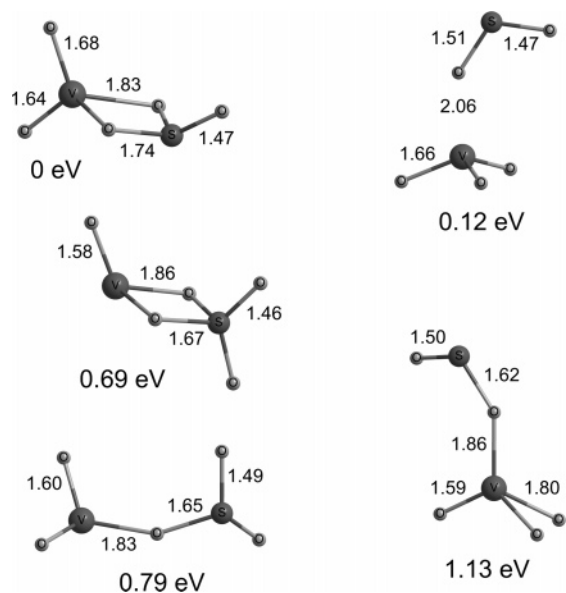


Figure 7. VO_3SO_2 structures computed at the BPW91/TZVP level of theory.

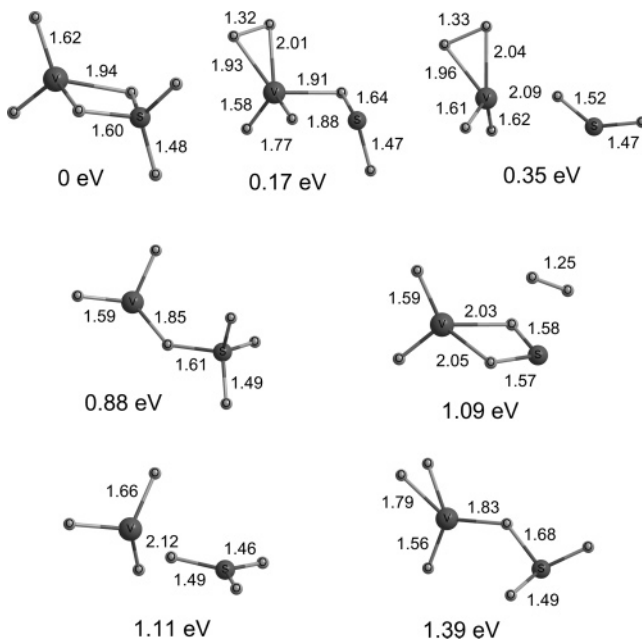


Figure 8. VO_4SO_2 structures computed at the BPW91/TZVP level of theory.

theory. Despite the shortcomings of this method, calculations can still provide us with valuable insights into the reaction mechanisms. As the oxidation of SO_2 is suggested to require only one vanadium surface site,³² calculations focused on VO_y clusters should also be representative of a mechanism occurring on larger clusters.

Figure 9 shows one possible reaction path for ${}^4\text{VO} + {}^1\text{SO}_2 \rightarrow {}^2\text{VO}_2 + {}^3\text{SO}$. With the exception of the first step (association of VO and SO_2), this reaction path is computed on the doublet potential energy surface. The association of ${}^4\text{VO}$ with SO_2 , as well as ${}^2\text{VO}$ with SO_2 , is barrierless with a possible crossing point between the two surfaces. Calculations presented here are preliminary—further calculations considering both doublet and quartet potential energy reaction surfaces with the localization of all possible crossing points are necessary to get a complete picture of the molecular mechanism for this reaction. At this point, no overall barrier for the reaction is found, only small

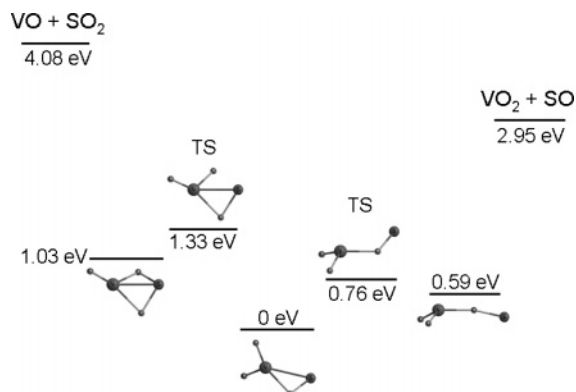


Figure 9. Possible reaction path for $\text{VO} + \text{SO}_2 \rightarrow \text{VO}_2 + \text{SO}$.

TABLE 4: Bonding Energies for Lowest Energy Isomers of VO_ySO_2 ($y = 1-4$) Clusters Computed at the BPW91/TZVP Level of Theory

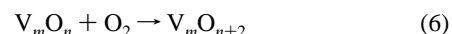
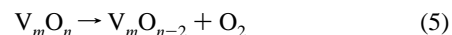
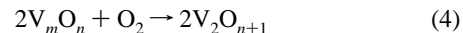
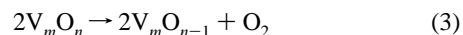
structure	bonding energy [eV]
$\text{VO} + \text{SO}_2$	4.08
$\text{VO}_2 + \text{SO}_2$	2.75
$\text{VO}_3 + \text{SO}_2$	1.51
$\text{VO}_4 + \text{SO}_2$	1.19

barriers for rearrangement of intermediate structures of $^2\text{VOSO}_2$. If a barrier to the above reaction is found for the quartet potential energy reaction surface, then this would only change the reaction rate constant; however, we do not observe the reaction intermediate VOSO_2 experimentally.³⁶ Note that due to the existence of many different isomers and electronic states of VOSO_2 , several possible reaction paths for formation of VO_2 and SO will exist.

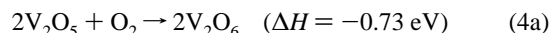
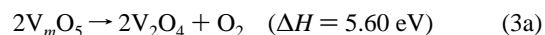
4.3. Condensed Phase Catalytic Mechanisms. On the basis of the calculations presented here, we can propose some possible catalytic mechanisms for $\text{SO}_2 \rightarrow \text{SO}_3$ catalytic conversion in the condensed phase. First of all, based on the gas-phase results, one specific vanadium oxide cluster does not appear to be responsible for the catalytic behavior of vanadium oxides. On the contrary, SO_2 will react with most clusters: reactions with oxygen deficient clusters will lead to the formation of SO , whereas reactions with oxygen rich clusters will result in the formation of SO_3 . SO can further react with O_2 to produce SO_3 ($\Delta H = -96$ kcal/mol, rate gas kinetic), providing another channel for formation of SO_3 .⁴⁹ Note that other processes, such as SO_2 formation, might compete with the SO_3 formation from SO .⁴⁹ Furthermore, “stable clusters” such as VO_2 , V_2O_5 , V_3O_7 , and V_4O_{10} are predicted to be least reactive with SO_2 . They will still form intermediate complexes with SO_2 (see also part I³⁶), but overall reactions of these clusters with SO_2 leading to the formation of SO or SO_3 are endothermic, requiring extra energy. Note that the general “belief” that catalytic reactions occur at defect condensed phase or surface sites is consistent with these results. In the following paragraphs, we will describe two possible catalytic cycles that rely on these oxidation/reduction properties of vanadium oxide clusters. In the following discussion, the calculated properties of oxygen deficient, oxygen rich, and stable clusters in the gas phase serve as a model for the properties of oxygen rich, oxygen deficient and stable sites in the condensed phase. V_mO_n denote the stable sites, while V_mO_{n+i} and V_mO_{n-i} (m, n, i are positive integers, $i < n$) describe oxygen rich and oxygen deficient sites, respectively. All general equations are numbered, with the equations describing some specific example bearing the number of the corresponding general equation followed by a letter (i.e., 1a). Enthalpy for

the specific reactions involving vanadium oxide clusters is given based on the calculations performed with gas-phase clusters at the BPW91/LANL2DZ level of theory. Enthalpy of SO_3 formation from SO is taken from available experimental data.⁴⁷

4.3.1. Catalytic Cycle 1: $\text{SO}_2 \rightarrow \text{SO}_3$ Occurs on Oxygen Rich or Oxygen Deficient Sites. Step #1: Formation of the oxygen rich and oxygen deficient sites from stable sites.

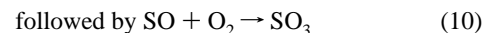
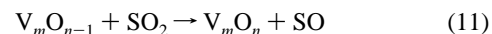
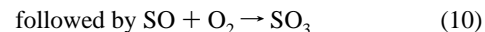
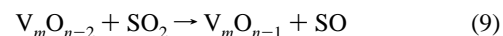
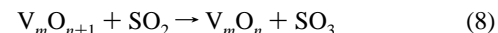
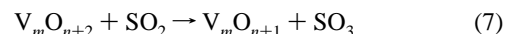


For example,

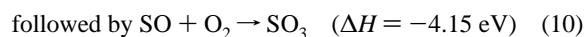
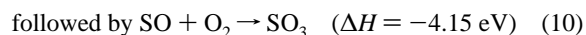
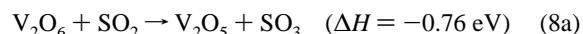
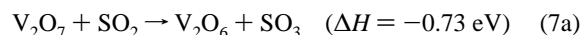


Oxygen deficient and oxygen rich sites are formed from the stable sites. This step is endothermic and requires some source of energy, for example in the form of heat. (Note that although reactions like $2\text{V}_2\text{O}_5 + \text{O}_2 \rightarrow 2\text{V}_2\text{O}_6$ are overall predicted to be exothermic, they will have a barrier as $\text{O}-\text{O}$ bond breaking requires some activation energy.) Additionally, some oxygen rich or oxygen deficient sites (or defects) will be naturally present in the condensed phase.

Step #2: Reactions of oxygen deficient and oxygen rich sites with SO_2 , regeneration of stable sites.

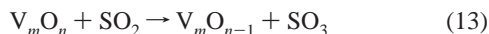
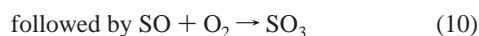
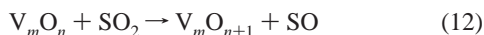


For example,

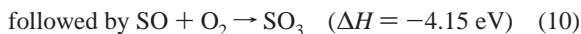


Oxygen deficient and oxygen rich sites react with SO_2 , leading to the formation of SO and SO_3 . SO further reacts with O_2 , producing SO_3 . These reactions are exothermic and without significant barriers. Stable sites are also regenerated in this step, since oxygen rich sites are reduced and oxygen deficient oxidized.

4.3.2. Catalytic Cycle 2: $\text{SO}_2 \rightarrow \text{SO}_3$ Occurs on Stable Sites. Step #1: Reactions of stable sites with SO_2

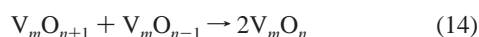
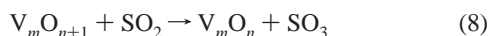


For example,

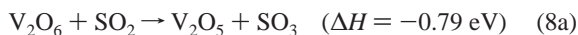


Stable sites react with SO_2 , producing SO_3 and SO as well as oxygen rich and oxygen deficient sites. These reactions are endothermic, requiring additional energy.

Step #2: Regeneration of stable sites



For example,



There are several ways by which stable sites can be regenerated in this step: (1) oxygen deficient and oxygen rich sites react with leftover SO_2 , producing SO_3 and a stable site; (2) oxygen deficient and oxygen rich sites react with each other, forming two stable sites; and (3) oxygen poor clusters are oxidized with O_2 present in the system.

In addition to the two mechanisms described above, other mechanisms leading to the SO_3 formation are possible. Experimental evidence exists for reaction of stable sites with SO_2 and O_2 leading to the formation of oxygen rich sites and SO_3 . This mechanism is discussed in more detail in part II.³⁶ One can imagine other mechanisms as well—for example, two units of SO_2 coming together on a vanadium oxide, producing SO and SO_3 [a $V_2O_4(SO_2)_2$ complex has also been experimentally observed³⁶]. Additional mechanisms, involving first reduction of a vanadium oxide by SO_2 and then its reoxidation by O_2 ,³¹ or adsorption of O_2 followed by oxidation of two SO_2 molecules,¹ have been suggested based on condensed-phase experimental work. Which one of these mechanisms most closely describes actual processes occurring in the condensed phase should be a subject of further experimental and theoretical studies. Note, however, that the profusion of potential mechanisms is a positive and perhaps important part of the overall efficiency of the catalytic conversion of SO_2 to SO_3 by vanadium oxide. In general, catalytic metal oxide surfaces are very complex and can terminate with multiple surface functionalities.⁵⁰ Moreover, vanadium oxide catalytic conversion of SO_2 to SO_3 occurs in the molten phase under high temperatures and presence of alkali metal sulfates,⁵¹ which leads to formation of a variety of chemical species and adds yet another layer of complexity. Quite possibly, no single mechanism is responsible

for the catalytic formation of SO_3 , but two or more mechanisms occur concurrently, thus making vanadium oxide a very efficient catalyst.

5. Conclusions

Reactions of neutral vanadium oxide clusters with SO_2 are studied with the aim of elucidating a mechanism for catalytic formation of SO_3 . Theoretical calculations at the BPW91/LANL2DZ level of theory, calibrated with the experimental enthalpies of formation for SO_{1-3} molecules, suggest that both oxidation and reduction of SO_2 occur. $SO_2 \rightarrow SO_3$ formation takes place on the oxygen-rich clusters, whereas $SO_2 \rightarrow SO$ formation is facilitated by oxygen-poor vanadium oxide clusters. SO formation provides another channel for SO_3 production, as SO readily reacts with O_2 : $SO + O_2 \rightarrow SO_3$ (see eq 10, above). SO and SO_3 formation is also confirmed by gas-phase experimental studies.³⁶ Neutral vanadium oxide clusters form stable reaction intermediates with SO_2 , illustrated with the example of the smallest vanadium oxide clusters VO_y , $y = 1-4$. Furthermore, preliminary BPW91/TZVP calculations find no overall barrier for the $VO + SO_2 \rightarrow VO_2 + SO$ reaction, suggesting that reactions of oxygen poor clusters with SO_2 occur rather easily. In general, many possible reaction paths will be feasible because a variety of $V_xO_ySO_2$ isomers exist that are lower in energy than the reactants or products. Finally, two possible catalytic cycles are suggested based on the facility of vanadium oxide clusters both to oxidize and reduce SO_2 . We suggest that more than just one detailed mechanism contributes to the conversion of SO_2 to SO_3 in the condensed phase. Further experimental and theoretical work is necessary to determine the role played by specific mechanisms.

Reported calculations are in very good agreement with and complement gas-phase molecular beam experimental studies of neutral vanadium oxide clusters. One general extrapolation from these studies of heterogeneous catalysis can be suggested concerning the overall oxidation/reduction catalytic processes we have posited: the profusion of the reactant species, reaction intermediates and transition states, and even mechanisms for the conversion of SO_2 to SO_3 may be major reasons that vanadium oxide is an excellent oxidation/reduction catalyst for the reaction. The fact that many low-lying, energy-accessible reaction intermediates and transition states are available, that many sites (clusters) can initiate the conversion, that many paths can lead to SO or SO_3 , and that the thermodynamics enable and favor both product generation and catalyst regeneration to occur, ensure an overall very efficient and general rate enhancement process for the reaction.

Acknowledgment. This research is supported in part by the US DOE (BES) and Phillip Morris USA, as well as by the National Science Foundation through the San Diego Supercomputer Center under Grant No. CHE060029 using IBM p-Series 655, and IBM p-Series 690, and the National Center for Supercomputing Applications under grant CHE060002 using IBM p-Series 690. Authors also thank Professor Anthony K. Rappé for helpful comments and discussions.

References and Notes

- (1) Lapina, O. B.; Bal'zhinimaev, B. S.; Boghosian, S.; Eriksen, K. M.; Fehrmann, R. *Catal. Today* **1999**, *51* (3-4), 469.
- (2) Oyama, S. T.; Somorjai, G. A. *J. Phys. Chem.* **1990**, *94* (12), 5022.
- (3) Bond, G. C.; Tahir, S. F. *Appl. Cat.* **1991**, *71* (1), 1.
- (4) Wu, H. B.; Wang, L. S. *J. Chem. Phys.* **1998**, *108* (13), 5310. Zhai, H. J.; Wang, L. S. *J. Chem. Phys.* **2002**, *117* (17), 7882.

- (5) Asmis, K. R.; Meijer, G.; Brummer, M.; Kaposta, C.; Santambrogio, G.; Woste, L.; Sauer, J. *J. Chem. Phys.* **2004**, *120* (14), 6461. Asmis, K. R.; Santambrogio, G.; Brummer, M.; Sauer, J. *Angew. Chem., Int. Ed.* **2005**, *44* (20), 3122.
- (6) Knight, L. B.; Babb, R.; Ray, M.; Banisaukas, T. J.; Russon, L.; Dailey, R. S.; Davidson, E. R. *J. Chem. Phys.* **1996**, *105* (23), 10237.
- (7) Zhao, Y. Y.; Gong, Y.; Chen, M. H.; Zhou, M. F. *J. Phys. Chem.* **2006**, *A 110* (5), 1845.
- (8) Pykavy, M.; van Wullen, C. *J. Phys. Chem. A* **2003**, *107* (29), 5566.
- (9) Pykavy, M.; van Wullen, C.; Sauer, J. *J. Chem. Phys.* **2004**, *120* (9), 4207.
- (10) Vyboishchikov, S. F.; Sauer, J. *J. Phys. Chem. A* **2000**, *104* (46), 10913.
- (11) Calatayud, M.; Andres, J.; Beltran, A. *J. Phys. Chem. A* **2001**, *105* (42), 9760.
- (12) Fielicke, A.; Rademann, K. *Phys. Chem. Chem. Phys.* **2002**, *4* (12), 2621.
- (13) Feyel, S.; Schroder, D.; Schwarz, H. *J. Phys. Chem. A* **2006**, *110* (8), 2647. Bell, R. C.; Zemski, K. A.; Kerns, K. P.; Deng, H. T.; Castleman, A. W. *J. Phys. Chem. A* **1998**, *102* (10), 1733. Moore, N. A.; Mitric, R.; Justes, D. R.; Bonacic-Koutecky, V.; W. Castleman, A. *J. Phys. Chem. B* **2006**, *110* (7), 3015. Justes, D. R.; Castleman, A. W.; Mitric, R.; Bonacic-Koutecky, V. *European Physical Journal D* **2003**, *24* (1–3), 331. Justes, D. R.; Mitric, R.; Moore, N. A.; Bonacic-Koutecky, V.; Castleman, A. W. *J. Am. Chem. Soc.* **2003**, *125* (20), 6289.
- (14) Feyel, S.; Scharfenberg, L.; Daniel, C.; Hartl, H.; Schroder, D.; Schwarz, H. (2007).
- (15) Vyboishchikov, S. F. *J. Mol. Struct.—Theochem.* **2005**, *723* (1–3), 53.
- (16) Anstrom, M.; Topsoe, N. Y.; Dumesic, J. A. *J. Catal.* **2003**, *213* (2), 115.
- (17) Gracia, L.; Sambrano, J. R.; Safont, V. S.; Calatayud, M.; Beltran, A.; Andres, J. *J. Phys. Chem. A* **2003**, *107* (17), 3107. Gracia, L.; Andres, J.; Safont, V. S.; Beltran, A. *Organometallics* **2004**, *23* (4), 730.
- (18) de Noronha, A. L. O.; Duarte, H. A. *J. Inorg. Biochem.* **2005**, *99* (8), 1708.
- (19) Gijzeman, O. L. J.; van Lingen, J. N. J.; van Lenthe, J. H.; Tinnemans, S. J.; Keller, D. E.; Weckhuysen, B. M. *Chem. Phys. Lett.* **2004**, *397* (1–3), 277.
- (20) Keller, D. E.; Koningsberger, D. C.; Weckhuysen, B. M. *J. Phys. Chem. B* **2006**, *110* (29), 14313. van Lingen, J. N. J.; Gijzeman, O. L. J.; Weckhuysen, B. M.; van Lenthe, J. H. *J. Catal.* **2006**, *239* (1), 34.
- (21) Schoiswohl, J.; Surnev, S.; Netzer, F. P.; Kresse, G. *J. Phys.: Condens. Matter.* **2006**, *18* (4), R1.
- (22) Vyboishchikov, S. F.; Sauer, J. *J. Phys. Chem. A* **2001**, *105* (37), 8588.
- (23) Brazdova, V.; Ganduglia-Pirovano, M. V.; Sauer, J. *Phys. Rev. B* **2004**, *69* (16).
- (24) Khaliullin, R. Z.; Bell, A. T. *J. Phys. Chem. B* **2002**, *106* (32), 7832. Dobler, J.; Pritzsche, M.; Sauer, J. *J. Am. Chem. Soc.* **2005**, *127* (31), 10861.
- (25) Redfern, P. C.; Zapol, P.; Sternberg, M.; Adiga, S. P.; Zygmont, S. A.; Curtiss, L. A. *J. Phys. Chem. B* **2006**, *110* (16), 8363.
- (26) Ganduglia-Pirovano, M. V.; Sauer, J. *J. Phys. Chem. B* **2005**, *109* (1), 374.
- (27) Ganduglia-Pirovano, M. V.; Sauer, J. *Phys. Rev. B* **2004**, *70* (20). Ganduglia-Pirovano, M. V.; Sauer, J. *Phys. Rev. B* **2004**, *70* (4).
- (28) Tokarz-Sobieraj, R.; Grybos, R.; Witko, M.; Hermann, K. *Collect. Czech. Chem. Commun.* **2004**, *69* (1), 121. Tokarz-Sobieraj, R.; Witko, M.; Grybos, R. *Catal. Today* **2005**, *99* (1–2), 241.
- (29) Abu Haija, M.; Guimond, S.; Romanyshyn, Y.; Uhl, A.; Kuhlenbeck, H.; Todorova, T. K.; Ganduglia-Pirovano, M. V.; Dobler, J.; Sauer, J.; Freund, H. *J. Surf. Sci.* **2006**, *600* (7), 1497.
- (30) Kato, A.; Seiyama, T.; Tomoda, K.; Mochida, I. *Bull. Chem. Soc. Jpn.* **1972**, *45* (3), 690.
- (31) Dunn, J. P.; Koppula, P. R.; Stenger, H. G.; Wachs, I. E. *Appl. Catal. B-Environ.* **1998**, *19* (2), 103.
- (32) Dunn, J. P.; Stenger, H. G.; Wachs, I. E. *Catal. Today* **1999**, *51* (2), 301. Dunn, J. P.; Stenger, H. G.; Wachs, I. E. *J. Catal.* **1999**, *181* (2), 233. Dunn, J. P.; Stenger, H. G.; Wachs, I. E. *Catal. Today* **1999**, *53* (4), 543.
- (33) Fouda, M. F. R.; Saleh, H. I.; Abd-Elzaher, M. M.; Amin, R. S. *Appl. Catal. A – Gen. I.* **2002**, *223* (1–2), 11.
- (34) Giakoumelou, I.; Caraba, R. M.; Parvulescu, V. I.; Boghosian, S. *Catal. Lett.* **2002**, *78* (1–4), 209.
- (35) Giakoumelou, L.; Parvulescu, V.; Boghosian, S. *J. Catal.* **2004**, *225* (2), 337.
- (36) He, S. G.; Xie, Y.; Dong, F.; Heinbuch, S.; Jakubikova, E.; Rocca, J. J.; Bernstein, E. R. Paper II, in preparation.
- (37) Muetterties, E. L. *Science* **1977**, *196* (4292), 839.
- (38) Becke, A. D. *J. Chem. Phys.* **1993**, *98* (7), 5648. Lee, C. T.; Yang, W. T.; Parr, R. G. *Phys. Rev. B* **1988**, *37* (2), 785.
- (39) Foltin, M.; Stueber, G. J.; Bernstein, E. R. *J. Chem. Phys.* **2001**, *114* (20), 8971.
- (40) Becke, A. D. *Phys. Rev. A* **1988**, *38* (6), 3098. Perdew, J. P.; Wang, Y. *Phys. Rev. B* **1992**, *45* (23), 13244.
- (41) Jakubikova, E.; Rappe, A. K.; Bernstein, E. R. *J. Phys. Chem. A* **2007**, accepted.
- (42) Hay, P. J.; Wadt, W. R. *J. Chem. Phys.* **1985**, *82* (1), 270.
- (43) Dunning, Jr. T. H.; Hay, P. J. in *Modern Theoretical Chemistry*, edited by H. F. Schaefer (Plenum Press, New York, 1976), Vol. 3.
- (44) *NIST Chemistry WebBook, NIST Standard Reference Database Number 69*, edited by P. J. Linstrom and W. G. Mallard (National Institute of Standards and Technology, Gaithersburg MD, June 2005).
- (45) Frisch, M. J.; Trucks, G. W.; Schlegel, H. B.; Scuseria, G. E.; Robb, M. A.; Cheeseman, J. R.; Zakrzewski, V. G.; Montgomery, J. J. A., R. E.; Stratmann, J. C.; Burant, S.; Dapprich, J. M.; Millam, A. D.; Daniels, K. N.; Kudin, M. C.; Strain, O.; Farkas, J.; Tomasi, V.; Barone, M.; Cossi, R.; Cammi, B.; Mennucci, C.; Pomelli, C.; Adamo, S.; Clifford, J. W.; Ochterski, G. A.; Petersson, P. Y.; Ayala, Q.; Cui, K.; Morokuma, P.; Salvador, J. J.; Dannenberg, D. K.; Malick, A. D.; Rabuck, K.; Raghavachari, J. B.; Foresman, J.; Cioslowski, J. V.; Ortiz, A. G.; Baboul, B. B.; Stefanov, G.; Liu, A.; Liashenko, P.; Piskorz, I.; Komaromi, R.; Gomperts, R. L.; Martin, D. J.; Fox, T.; Keith, M. A.; Al-Laham, C. Y.; Peng, A.; Nanayakkara, M.; Challacombe, P. M. W.; Gill, B.; Johnson, W.; Chen, M. W.; Wong, J.; Andres, C.; Gonzalez, M.; Head-Gordon, E. S. Replogle, and Pople, J. A. *Gaussian 98, Revision A.11* (Gaussian, Inc., Pittsburgh PA, 2001).
- (46) Balducci, G.; Gigli, G.; Guido, M. *J. Chem. Phys.* **1983**, *79* (11), 5616.
- (47) *CRC Handbook of Chemistry and Physics*, 85th ed.; CRC Press: Boca Raton, FL, 2004.
- (48) Dunning, T. H.; Peterson, K. A.; Wilson, A. K. *J. Chem. Phys.* **2001**, *114* (21), 9244. Bell, R. D.; Wilson, A. K. *Chem. Phys. Lett.* **2004**, *394* (1–3), 105. Wilson, A. K.; Dunning, T. H. *J. Chem. Phys.* **2003**, *119* (22), 11712. Yockel, S.; Wilson, A. K. *Chem. Phys. Lett.* **2006**, *429* (4–6), 645.
- (49) Wood, W. P.; Heicklen, J. *J. Phys. Chem.* **1971**, *75* (7), 861.
- (50) Wachs, I. E. *Catal. Today* **2005**, *100* (1–2), 79.
- (51) Dearnaley, R. I.; Kerridge, D. H. *Thermochim. Acta* **1987**, *121*, 121. West, J. R.; Smith, G. M. In *Riegel's Handbook of Industrial Chemistry*; Kent, J. A., Ed; Van Nostrand Reinhold Company Inc.: New York, 1983; p 130.
- (52) Pedley, J. B.; Marshall, E. M. *J. Phys. Chem. Ref. Data* **1983**, *12* (4), 967.
- (53) Huber, K. P.; Herzberg, G. *Molecular Spectra and Molecular Structure. IV. Constants of Diatomic Molecules*; Van Nostrand Reinhold: New York, 1979.
- (54) Li, J.; Demello, P. C.; Jug, K. *J. Comput. Chem.* **1992**, *13* (1), 85.
- (55) Rakowitz, F.; Marian, C. M.; Seijo, L. *J. Chem. Phys.* **1999**, *111* (23), 10436.